Quantum Enhanced Optical Phase Estimation With a Squeezed Thermal State

Juan Yu,[1] Yue Qin,[1] Jinliang Qin,[1,2] Hong Wang,[1] Zhihui Yan,[1,2,*] Xiaojun Jia,[1,2,†] and Kunchi Peng[1,2]

[1] *State Key Laboratory of Quantum Optics and Quantum Optics Devices, Institute of Opto-Electronics, Shanxi University, Taiyuan 030006, People's Republic of China*

[2] *Collaborative Innovation Center of Extreme Optics, Shanxi University, Taiyuan 030006, People's Republic of China*

(Received 3 December 2019; revised manuscript received 19 January 2020; accepted 24 January 2020; published 14 February 2020)

Quantum phase-estimation protocols can provide a measuring method of phase shift with precision superior to the standard quantum limit (SQL) due to the application of a nonclassical state of light. A squeezed vacuum state, whose variance in one quadrature is lower than the corresponding SQL, has been pointed out as a sensitive resource for quantum phase estimation and the estimation accuracy is directly influenced by the properties of the squeezed state. Here we analyze in detail the influence of the purity and squeezing level of the squeezed state on the accuracy of quantum phase estimation. The maximum precision that can be achieved for a squeezed thermal state is evaluated, and the experimental results are in agreement with the theoretical analyses. It is also found that the width of the phase-estimation interval $\Delta\theta$ beyond SQL is correlated with the purity of the squeezed state.

DOI: 10.1103/PhysRevApplied.13.024037

I. INTRODUCTION

The question of measuring the phase of light has been a subject of great debate since the early work of Dirac [1]. Due to the inexistence of the phase Hermitian operator, the true value of phase cannot be directly measured. A general method is to find an observable Hermitian operator associated with phase, such as field- or intensity-based quantities by interferometric devices [2–7], and then deduce the phase indirectly according to the measurement results. This indirect measurement process for the value of phase shift is called phase estimation. The accuracy of usual phase estimation is limited by the standard quantum limit (SQL) because of the vacuum fluctuation of quantized electromagnetic field [8]. Phase estimation is a powerful measurement strategy to perform accurate measurements of various physical quantities including length, velocity, and displacements [9,10], and it is the heart of many quantum-enhanced metrology applications, such as improvement of time and frequency standards [11,12], gravitational-wave detection [13,14], interferometry based on interacting systems [15,16], quantum imaging [17–19], atomic clock [20], and magnetometry [21–24].

Since Caves proposed that a quantum state can break the limit of shot noise in 1981 [25], many optical systems [26–35] have proved that a real quantum state, for instance a squeezed state and an entangled state, can greatly improve the accuracy of phase estimation with a given average photon number [36,37]. The accuracy of phase estimation is influenced by the properties of the quantum state. In the basic principle of quantum optics, the fluctuation added in one quadrature should be equal to that reduced in its orthogonal quadrature for an ideal squeezed state of light. However, a realistic squeezed state is difficult to be exactly pure especially for high-level squeezed state due to the existence of extra noise in its generation system [38]. Accordingly, it is quite necessary to explore the effect of the properties of the squeezed state on the phase-estimation results.

The theory of quantum phase estimation provides the ultimate bound on precision of phase estimation in the form of quantum Cramér-Rao bound (QCRB), which is independent with detection strategies [39]. The QCRB is essentially determined by Heisenberg uncertainty and is given by the inverse of quantum Fisher information (QFI) associated with the resource. The theoretical analyses show that homodyne measurement is optimal for squeezed pure state but not optimal for squeezed thermal state, and the maximum precision that can be achieved for squeezed thermal state via homodyne measurement is called optimal Cramér-Rao bound (OCRB) [40]. In Ref. [41], a squeezed-enhanced phase estimation is realized with the help of feedback control. Here, we analyze in detail the influence of properties of squeezed state on the phase estimation results. By using a squeezed thermal state as the probe

*zhyan@sxu.edu.cn
†jiaxj@sxu.edu.cn

beam, the effects of the squeezing level and the purity of a squeezed state on the phase-estimation results are given. Then, we experimentally implement the quantum phase estimation because it can be enhanced with a much higher squeezing level and the squeezed pure state behaves as the optimal resource to reach QCRB. Our research is of general interest in the sense that the phase estimation is based on the squeezing mechanism and the results provide a reference for multiphase estimation based on multipartite entanglement [42,43].

II. PHASE ESTIMATION WITH A SQUEEZED THERMAL STATE

An optical field can be represented by the annihilation operator $\hat{a}$ in quantum mechanics. The orthogonal amplitude and phase operators can be represented in terms of the creation and annihilation operators as $\hat{x} = \left(\hat{a} + \hat{a}^{\dagger}\right)/\sqrt{2}$ and $\hat{p} = i\left(\hat{a}^{\dagger} - \hat{a}\right)/\sqrt{2}$, $\hat{x}$ and $\hat{p}$ satisfy the commutation relations $\left[\hat{x}, \hat{p}\right] = i$. Usually, a coherent state or a vacuum state is a minimum uncertainty state and the variances of the two quadrature components are equal: $\langle \Delta^2 \hat{x} \rangle = \langle \Delta^2 \hat{p} \rangle = 1/2$. A squeezed state is defined as its variance of one quadrature is reduced relative to the corresponding SQL while the variance of its orthogonal quadrature is amplified. The squeezing parameter r is used to indicate the squeezing level of the squeezed state, i.e., the variance in a squeezed quadrature, $e^{-2r}/2$, is always below the corresponding SQL [44]. The mean photon number of pure squeezed vacuum state is $n = \sinh^2 r$. In the past decades, squeezed states of light have been obtained by several groups and squeezing level has been improved continually [45–48]. In the actual experimental generation processing, there is some inevitably extra noise in its antisqueezing quadrature component. An extra-antisqueezing parameter r' is introduced to describe the extra noise level of the antisqueezing quadrature component [49] and the covariance matrix of this squeezed state is expressed as $\boldsymbol{\sigma}_0 = 1/2\ \mathrm{Diag}(e^{-2r}, e^{2r+2r'})$, which is usually called a squeezed thermal state. The mean photon number of squeezed thermal state is $n = e^{r'} n_r + (e^{r'} - 1)/2$, where $n_r = \sinh^2(r + r'/2)$ is the photon number contributing from the squeezing effect, $(e^{r'} - 1)/2$ is the photon number contributing from the extra noise in antisqueezing quadrature [40].

A general scheme of a quantum phase estimation with a squeezed state is shown in Fig. 1. A squeezed state $\hat{\rho}\,(0)$ undergoes a phase shift described by a unitary operator $\hat{U}(\theta) = \exp\left(-i\theta\hat{n}\right)$,

$$\hat{\rho}\,(\theta) = \hat{U}(\theta)\,\hat{\rho}\,(0)\,\hat{U}^{\dagger}(\theta)\,, \tag{1}$$

where $\hat{n} = \hat{a}^{\dagger}\hat{a}$ is a number operator and θ is the phase shift to be estimated. The output state is detected by a detection strategy and the obtained data samples associated with the phase shift are processed by Bayesian inference [50]. The

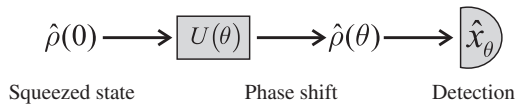

FIG. 1. Schematic of a general quantum phase estimation. A squeezed state $\hat{\rho}\,(0)$ undergoes an unknown phase shift θ. A function of the data samples $\hat{x}_\theta$ associated with the phase shift are measured by a detection strategy.

essence of phase-shift operation is a rotation operation on an initial state, and the quadrature operator is expressed as $\hat{x}_\theta = \left(\hat{a}e^{-i\theta} + \hat{a}^{\dagger}e^{i\theta}\right)/\sqrt{2}$. The variance of the squeezed state $\hat{\rho}\,(\theta)$ is associated with the phase shift acted on the probe beam, and the phase shift can be indirectly obtained by measuring the variance of quadrature $\hat{x}_\theta$ via homodyne detection. Thus, the phase-estimation protocol we provide here is only appropriate for a squeezed state. In general, the variance of phase shift $\mathrm{Var}[\theta]$ for any unbiased estimator is bounded at the times of measurements N by the Cramér-Rao theorem [51]:

$$\mathrm{Var}\,[\theta] \geq \frac{1}{NF\,(\theta)}, \tag{2}$$

where $F\,(\theta)$ is the Fisher information (FI) [52], which is the observed information about the unknown parameter. The QFI H is the maximized FI over all possible detection schemes, i.e., $F\,(\theta) \leq H$. According to Ref. [53], H can be fully expressed in terms of the covariance matrix of the Gaussian state and the QCRB of the quantum phase estimation for a single-mode squeezed thermal state is

$$\mathrm{Var}_{\mathrm{sq}}\,[\theta] = \frac{1}{8Nn_r\,(n_r+1)}\left[\frac{1}{2} + \frac{1}{2}e^{-2r'}\right]. \tag{3}$$

In comparison with a coherent state to be used as the probe beam in the phase estimation [approximately $1/\,(4Nn)$, where n is the mean photon number of probe beam] [40], the estimation accuracy can be greatly improved with the help of a squeezed state. For a squeezed pure state, there is no extra noise in the antisqueezing quadrature component, i.e., $r' = 0$, and the QCRB becomes $\mathrm{Var}\,[\theta] = 1/[8Nn_r\,(n_r+1)]$ [36,54,55].

III. REACHABLE BOUND WITH HOMODYNE DETECTION AND BAYESIAN INFERENCE

Homodyne detection is a common detection strategy for state reconstruction in the continuous-variable (CV) regime [56]. It is a kind of simple and accurate detection strategy because it can provide a phase reference for estimating the value of the phase shift. The data samples $\{\hat{x}_\theta\}$ associated with the phase shift θ are obtained through a local projective Von Neuman measurement and then the true value of phase shift can be indirectly deduced according to the measurement results [57].

In order to evaluate the maximum precision that is achieved for a squeezed thermal state with homodyne measurement, we use the Wigner function to describe our system [58–60]. In the Wigner function description, the quadratures of the probe beam correspond to two phase-space coordinates x and p, which can be grouped into a two-dimensional vector $\mathbf{X}$, $\mathbf{X}^T = (x, p)$. The Wigner function associated with the shifted squeezed thermal state $\hat{\rho}_{\beta,r}(\theta)$ is

$$W_\theta(\mathbf{X}) = \frac{\exp\left[-\frac{1}{2}\mathbf{X}^T\boldsymbol{\sigma}_\theta^{-1}\mathbf{X}\right]}{2\pi\sqrt{\mathrm{Det}[\boldsymbol{\sigma}_\theta]}}, \tag{4}$$

where $\boldsymbol{\sigma}_\theta$ is the covariance matrix after the phase shift,

$$\sigma_\theta = \frac{1}{2}\begin{bmatrix} e^{-2r}\cos^2\theta + e^{2r+2r'}\sin^2\theta & \frac{1}{2}(e^{2r+2r'} - e^{-2r})\sin(2\theta) \\ \frac{1}{2}(e^{2r+2r'} - e^{-2r})\sin(2\theta) & e^{2r+2r'}\cos^2\theta + e^{-2r}\sin^2\theta \end{bmatrix}. \tag{5}$$

Then the individual marginal probability distribution $p(x|\theta)$ conditioned on a single homodyne-measurement outcome of a shifted squeezed thermal state is calculated from the Wigner function [61]:

$$p(x|\theta) = \int_{\mathbb{R}} W_\theta(\mathbf{X})\, dy = \frac{1}{e^{r'}\sqrt{\pi\,\Sigma_\theta^2}}\exp\left[-\frac{x_\theta^2}{e^{2r'}\Sigma_\theta^2}\right], \tag{6}$$

where $\Sigma_\theta^2 = [e^{-2r-2r'}\cos^2\theta + e^{2r}\sin^2\theta]$ is the variance of the probe beam, $\{x_\theta\}$ is the noise distribution of the squeezed state associated with θ obtained from the homodyne measurement. The FI can be easily evaluated from its definition [62]:

$$\begin{aligned} F(\theta) &= \int_{\mathbb{R}} p(x|\theta)\left[\frac{\partial \log p(x|\theta)}{\partial\theta}\right]^2 dx \\ &= \frac{\sin^2(2\theta)\left(e^{2r} - e^{-2r-2r'}\right)^2}{2\left(\Sigma_\theta^2\right)^2}. \end{aligned} \tag{7}$$

It is obvious that the expression of the FI is dependent on the phase shift θ and the squeezing parameters r as well as the extra-antisqueezing parameter r'. The maximum of the FI can be achieved at an optimal phase $\theta_{\mathrm{opt}} = 1/2\arccos[\tanh(2r + r')]$ and $F_{\max}$ with homodyne measurement is

$$F_{\max} = 2\sinh^2(2r + r'). \tag{8}$$

Then upon using the Cramér-Rao theorem, the variance of optimal phase estimation with homodyne measurement goes as

$$\mathrm{Var}_{\mathrm{sq}}^{\mathrm{hom}}[\theta] = \frac{1}{8Nn_r(n_r+1)}. \tag{9}$$

It means that the homodyne measurement is not optimal for a squeezed thermal state by comparing Eqs. (3) and (9) and the estimation accuracy can attain the OCRB [41].

Bayesian inference, which is known as "probability theory," is the theory of how to combine uncertain information from multiple sources to make optimal decision under uncertainty. If x is the variable associated with the phase shift, then Bayes' rule states

$$p(\theta|x) = \frac{p(x|\theta)\,p(\theta)}{p(x)}, \tag{10}$$

where $p(\cdot|\cdot)$ are the conditional probabilities about parameters x and θ. $p(x|\theta)$ is the marginal probability distribution of the shifted squeezed thermal state and $p(\theta|x)$ is the *posteriori* probability distribution (PPD) of the phase shift. $p(x)$ are the total probabilities to observe x and $p(\theta) = 2/\pi$ is the prior information, which is a flat distribution. The result of each measurement is used as prior information for the next measurement. The PPD $p(\theta|x)$ based on N sampled homodyne measurements is given by

$$p(\theta|x) = \frac{1}{\mathcal{N}}\prod_{k=1}^{N} p(x_k|\theta), \tag{11}$$

where $\mathcal{N} = \int_0^{\pi/2} p(\theta|x)\,\theta$ is a normalization constant, $p(x_k|\theta)$ is the individual marginal probability distribution conditioned on each homodyne measurement, which are given by Eq. (6).

IV. EXPERIMENTAL SETUP AND RESULT

A schematic of the experimental setup is illustrated in Fig. 2, which includes a source of squeezed state, a balanced homodyne detection system, a phase control system, and a data acquisition system. A squeezed state is produced by a nondegenerate optical parametric amplifier (NOPA), which is pumped by a continuous wave intracavity frequency-doubled tunable single-frequency Nd:YAP/LBO solid-state laser provided by YuGuang company CDPSSFG-VIB (not shown in Fig. 2). The output fundamental wave at a wavelength of 1080 nm is used for the injected seed beams of NOPA and the local oscillator beam of homodyne detection system. The second harmonic wave at 540 nm serves as the pump field of the NOPA. The NOPA consists of an α-cut KTP crystal and a concave mirror, which can realize type-II noncritical phase matching without walk-off effect. The front face of the crystal is highreflection (HR) coated for 1080 nm and $T_1 = 18\%$ coated for 540 nm, which serves as the input coupler. The end face of the KTP is cut to 1° along the y-z plane of the crystal and is antireflection coated for both 1080 and 540 nm. The concave mirror with a radius of curvature of 50 mm coated with $T_2 = 12.5\%$ for 1080 nm and HR for 540 nm serves as the output coupler, which is mounted on a piezoelectric transducer to actively lock the cavity length of NOPA on resonance with the injected signal at 1080 nm. Through an intracavity frequency down-conversion processing in the NOPA, an Einstein-Podolsky-Rosen (EPR) entangled state of light or two single-mode squeezed states of light at 1080 nm with orthogonal polarizations can be generated separately [63]. The squeezed state with different squeezing parameter r and different purity can be generated by controlling the experimental conditions.

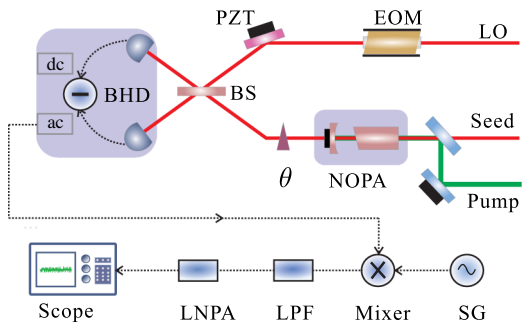

FIG. 2. Schematic of the experimental setup. Dotted curves and solid curves represent the circuitry part and the light path, respectively. NOPA, nondegenerate optical parametric amplifier; Pump, pump field of the NOPA; Seed, seed field of the NOPA; LO, a strong local oscillator beam; EOM, electro-optic modulator; PZT, piezo-electric transducer; BS, 50:50 beam splitter; BHD, balanced homodyne detector; dc, dc signal; ac, ac signal; SG, signal generator; θ, electric phase controller; LPF, low-pass filter; LNPA, low noise preamplifier; Scope, oscilloscope.

The generated squeezed state acquires an unknown phase shift θ within a range of $[0, \pi/2]$ and then is combined with a strong local oscillator beam (5 mW) at a 50:50 beam splitter (BS) for homodyne measurement. The relative phase control between the local oscillator beam and probe beam is achieved by an improved Pound-Drever-Hall (PDH) technique [64]. The local oscillator beam is phase modulated by an electro-optic modulator (EOM) with a sine signal at 7.3 MHz. The first-step error signal is obtained by mixing ac signal detected by the homodyne detector and the sine signal modulated on the EOM. The final error signal to realize the phase locking of probe beam and the local oscillator beam to a specific degree is obtained by coupling the first-step error signal with the dc output from the homodyne detector by a certain percentage. Finally, the error signal is fed back to the piezo-electric transducer (PZT) attached on a high-reflection mirror. The experimental data $\{x_\theta\}$ of quantum phase estimation is recorded by an oscilloscope via quantum tomography technique. A PPD of θ conditioned on the N-sampled homodyne measurements can be calculated according to Eq. (11).

To investigate the performance for different times of measurements N and squeezing parameter r, we fix the phase shift at $\theta = 0.4$ firstly in the experiment. The PPDs of the phase shift conditioned on the sampled homodyne data are obtained for different values of the involved parameters as a function of θ as shown in Fig. 3. The solid black, dash dot green, dot blue, and dash red curves correspond to $N = 1000, 500, 300, 100$, respectively. A suitable estimator for the actual value of a fixed phase shift is given by the maximum of the distribution because of the symmetric form of the PPD. The definition of the variance is $\mathrm{Var}[\theta] = \langle\theta^2\rangle - \langle\theta\rangle^2$, and the $\mathrm{Var}[\theta]$ is

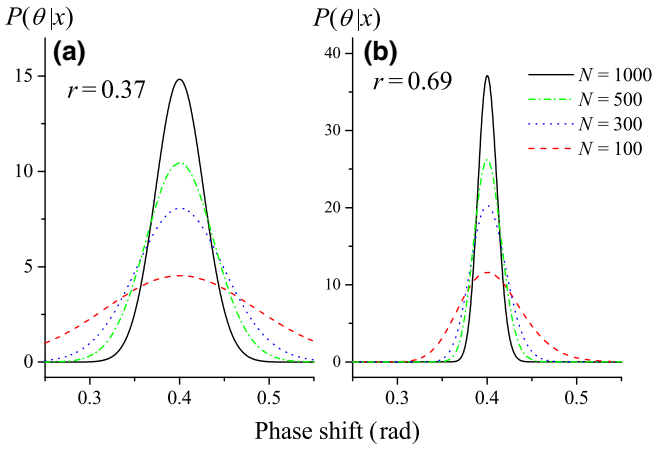

FIG. 3. *Posteriori* probability distributions for different values of the involved parameters at a fixed phase shift $\theta = 0.4$. (a),(b) PPDs versus phase shift for different numbers of homodyne samples N when the squeezing parameter r is 0.37 and 0.69, respectively.

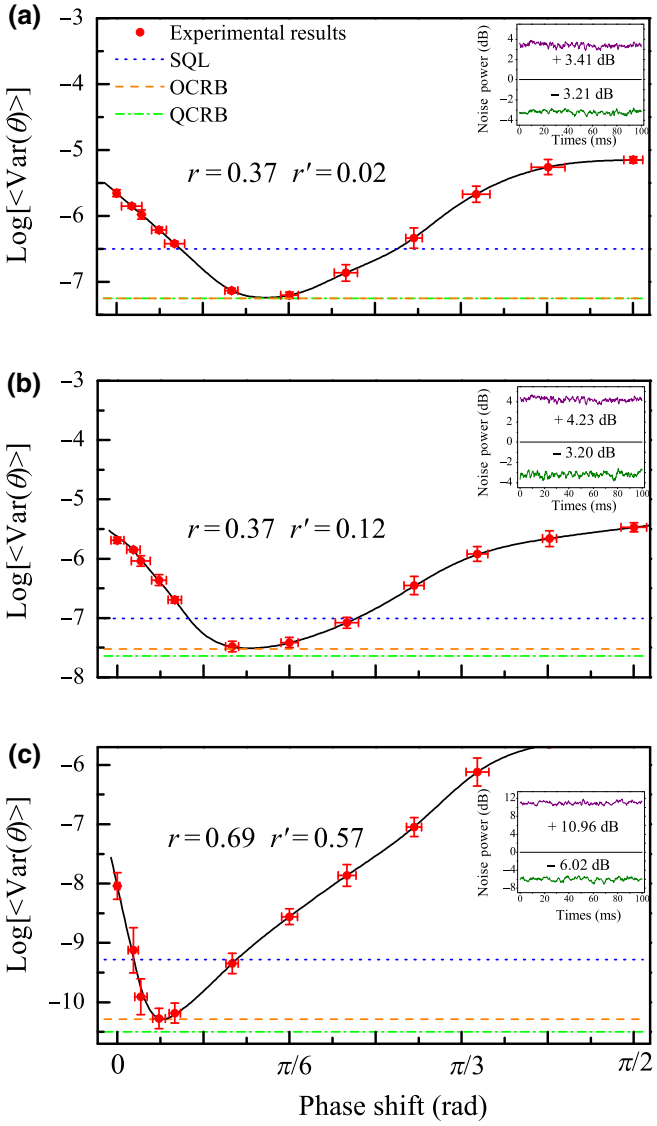

FIG. 4. Estimation variance versus phase shift for three different purity squeezed states as the probe beam. (a) The noise suppression of one quadrature is measured as −3.21 dB relative to the SQL while the noise of the orthogonal quadrature is amplified by +3.41 dB and the purity of the probe beam is 0.977. (b) The purity is 0.891 and the noise suppression of one quadrature is the same as (a) while the noise of the orthogonal quadrature is increased to +4.23 dB. (c) The purity is 0.566 and the measured noise levels are −6.02 dB and +10.96 dB. The estimation variances Var $[\theta]$ for 12 phase shifts in the $[0, \pi/2]$ range are marked as the red circles with the standard deviations over 20 repetitions. The dot blue, dash origin, and dash dot green curves correspond to the SQL, OCRB, and QCRB, respectively.

given by $1/NF(\theta)$, which is calculated from the homodyne measurements. Phase estimation can be enhanced with much higher squeezing parameter r and more times of measurements N.

Then we analyze the effect of the purity of probe beam on the accuracy of phase estimation. The estimation

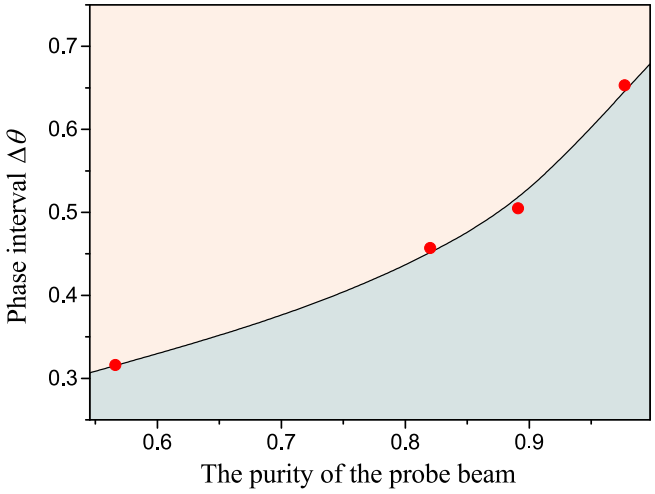

FIG. 5. The range of phase interval $\Delta\theta$ for the estimation variance beyond the SQL versus the purity of the probe beam. The red circles correspond to the experimental results.

variances Var $[\theta]$ for squeezed states with different purity are shown in Fig. 4. The estimation variances measured at 12 different phase shifts in $[0, \pi/2]$ range are marked as circles in the figure. The dot blue, dash origin, and dash dot green curves correspond to the SQL, OCRB, and QCRB, which is calculated with the corresponding equations with the same mean photon number, respectively. The noise power spectra of the probe beam at 3 MHz for different purity squeezed states measured by spectrum analyzers (SA) are shown in the insert of Fig. 4. It is obvious that the estimation accuracy attains OCRB only for one specific phase shift θ_{opt} and estimation accuracy beyond the SQL can be realized in a phase interval $\Delta\theta$ near the optimal phase shift θ_{opt} [59]. The larger the squeezing parameter r, the higher the estimation precision. Because the mean photon number of the probe beam is the main effect of the precision of quantum phase estimation, the estimation precision can also be enhanced by increasing the factor of the extra-antisqueezing parameter r' at the same r. For a squeezed state of the same squeezing level r, the mean photon number of the squeezed thermal state is more than that of the pure squeezed state because the existence of extra noise r' can increase the mean photon number of the squeezed state. Although the extra-antisqueezing parameter has a helpful influence on the absolute precision of phase estimation, the estimation accuracy is further away from the QCRB with the increase of r' due to the extra loss and phase fluctuation in antisqueezing quadrature. The accuracy of the quantum phase estimation can be enhanced with a much higher squeezing level at a given fixed mean photon number and squeezed pure state behaves as the optimal resource to reach QCRB, i.e., the Heisenberg limit asymptotically.

Finally, we analyze the influence of the purity of the probe beam on the phase interval $\Delta\theta$ of phase estimation beyond the SQL. The range of quantum phase estimation beyond the SQL for four different purity probe beams with different squeezing level are shown in Fig. 5. The $\Delta\theta$ increases with the purity of the probe beam. The range of $\Delta\theta$ is 0.653 at purity of squeezed state with 0.977, which is more than twice that at a purity of 0.566 without any feedback control.

V. CONCLUSION

Through analyzing in detail the influence of properties of squeezed thermal state on the precision of quantum phase estimation, it is found that the QCRB only can be reached with the help of a squeezed pure state and the absolute precision of quantum phase estimation can be enhanced with squeezed state of higher squeezing level. Through controlling the conditions of NOPA, squeezed states of light with different purity and squeezing level are used as a probe beam in the experiment of phase estimation. The experimental results are in good agreement with the theoretical analyses. This provides us with an alternative direction for a simple and convenient phase-estimation scheme and is also a good reference for the multiparameter estimation with a multipartite entanglement.

ACKNOWLEDGMENTS

The authors thank Kaimin Zheng and Shan Ma for helpful discussions. Our work is supported by the Key Project of the National Key R&D program of China (Grant No. 2016YFA0301402), the National Natural Science Foundation of China (Grants No. 61925503, No. 61775127, No. 11654002, No. 11804246, and No. 11834010), the Program for Sanjin Scholars of Shanxi Province, and the fund for Shanxi "1331 Project" Key Subjects Construction.

[1] P. A. M. Dirac, The quantum theory of the emission and zbsorption of radiation, Proc. R. Soc. A: Math. Phys. Eng. Sci. **114**, 243 (1927).
[2] H. M. Wiseman and G. J. Milburn, *Quantum Measurement and Control* (Cambridge University, England, 2010).
[3] G. Vittorio, L. Seth, and M. Lorenzo, Quantum-enhanced measurements: Beating the standard quantum limit, Science **306**, 1330 (2004).
[4] D. W. Berry and H. M. Wiseman, Adaptive quantum measurements of a continuously varying phase, Phys. Rev. A **65**, 043803 (2002).
[5] Z. Y. Ou, Fundamental quantum limit in precision phase measurement, Phys. Rev. A **55**, 2598 (1997).
[6] J. D. Zhang, Z. J. Zhang, L. Z. Cen, J. Y. Hu, and Y. Zhao, Nonlinear phase estimation: Parity measurement approaches the quantum Cramér-Rao bound for coherent states, Phys. Rev. A **99**, 022106 (2019).
[7] A. Lumino, E. Polino, A. S. Rab, G. Milani, N. Spagnolo, N. Wiebe, and F. Sciarrino, Experimental Phase Estimation Enhanced by Machine Learning, Phys. Rev. Appl. **10**, 044033 (2018).
[8] S. Boixo, M. J. Davis, and A. Shaji, Quantum Metrology: Dynamics versus Entanglement, Phys. Rev. Lett. **101**, 040403 (2008).
[9] V. Giovannetti, S. Lloyd, and L. Maccone, Advances in quantum metrology, Nat. Photonics **5**, 222 (2011).
[10] S. L. Braunstein and C. M. Caves, Statistical Distance and the Geometry of Quantum States, Phys. Rev. Lett. **72**, 3439 (1994).
[11] T. Udem, R. Holzwarth, and T. W. Hänsch, Optical frequency metrology, Nature **416**, 233 (2002).
[12] N. Hinkley, J. A. Sherman, N. B. Phillips, M. Schioppo, N. D. Lemke, K. Beloy, M. Pizzocaro, C. W. Oates, and A. D. Ludlow, An atomic clock with 10^{-18} instability, Science **341**, 1215 (2013).
[13] LIGO Scientific Collaboration, Enhanced sensitivity of the LIGO gravitational wave detector by using squeezed states of light, Nat. Photonics **7**, 613 (2013).
[14] U. L. Andersen, Quantum optics: Squeezing more out of LIGO, Nat. Photonics **7**, 589 (2013).
[15] J. A. Dunningham and K. Burnett, Sub-shot-noise-limited measurements with Bose-Einstein condensates, Phys. Rev. A **70**, 033601 (2004).
[16] M. F. Riedel, P. Böhi, Y. Li, T. W. Hänsch, A. Sinatra, and P. Treutlein, Atom-chip-based generation of entanglement for quantum metrology, Nature **464**, 1170 (2010).
[17] C. Lupo and S. Pirandola, Ultimate Precision Bound of Quantum and Subwavelength Imaging, Phys. Rev. Lett. **117**, 190802 (2016).
[18] M. Tsang, Quantum limit to subdiffraction incoherent optical imaging, Phys. Rev. A **99**, 012305 (2019).
[19] M. Ghalaii, M. Afsary, S. Alipour, and A. T. Rezakhani, Quantum imaging as an ancilla-assisted process tomography, Phys. Rev. A **94**, 042102 (2016).
[20] J. Sun, X. Zhang, W. Qu, E. E. Mikhailov, I. Novikova, H. Shen, and Y. H. Xiao, Spatial Multiplexing of Squeezed Light by Coherence Diffusion, Phys. Rev. Lett. **123**, 203604 (2019).
[21] S. Danilin, A. V. Lebedev, A. Vepsäläinen, G. B. Lesovik, G. Blatter, and G. S. Paraoanu, Quantum-enhanced magnetometry by phase estimation algorithms with a single artificial atom, npj Quantum Inf. **4**, 29 (2018).
[22] N. M. Nusran and M. V. Gurudev Dutt, Optimizing phase-estimation algorithms for diamond spin magnetometry, Phys. Rev. B **90**, 024422 (2014).
[23] J. R. Maze, P. L. Stanwix, J. S. Hodges, S. Hong, J. M. Taylor, P. Cappellaro, L. Jiang, M. V. G. Dutt, E. Togan, A. S. Zibrov, A. Yacoby, R. L. Walsworth, and M. D. Lukin, Nanoscale magnetic sensing with an individual electronic spin in diamond, Nature **455**, 644 (2008).
[24] J. M. Taylor, P. Cappellaro, L. Childress, L. Jiang, D. Budker, P. R. Hemmer, A. Yacoby, R. Walsworth, and M. D. Lukin, High-sensitivity diamond magnetometer with nanoscale resolution, Nat. Phys. **4**, 810 (2008).
[25] C. M. Caves, Quantum mechanical noise in an interferometer, Phys. Rev. D **23**, 1693 (1981).
[26] P. M. Anisimov, G. M. Raterman, A. Chiruvelli, W. N. Plick, S. D. Huver, H. Lee, and J. P. Dowling, Quantum

Metrology with Two-Mode Squeezed Vacuum: Parity Detection Beats the Heisenberg Limit, Phys. Rev. Lett. **104**, 103602 (2010).

[27] Z. X. Huang, K. R. Motes, P. M. Anisimov, J. P. Dowling, and D. W. Berry, Adaptive phase estimation with two-mode squeezed vacuum and parity measurement, Phys. Rev. A **95**, 053837 (2017).

[28] K. P. Seshadreesan, S. Kim, J. P. Dowling, and H. Lee, Phase estimation at the quantum Cramér-Rao bound via parity detection, Phys. Rev. A **87**, 043833 (2013).

[29] F. Liu, Y. Y. Zhou, J. Yu, J. L. Guo, Y. Wu, S. X. Xiao, D. Wei, Y. Zhang, X. J. Jia, and M. Xiao, Squeezing-enhanced fiber Mach-Zehnder interferometer for low-frequency phase measurement, Appl. Phys. Lett. **110**, 021106 (2017).

[30] B. L. Higgins, D. W. Berry, S. D. Bartlett, H. M. Wiseman, and G. J. Pryde, Entanglement-free Heisenberg-limited phase estimation, Nature **450**, 393 (2007).

[31] A. N. Boto, P. Kok, D. S. Abrams, S. L. Braunstein, C. P. Williams, and J. P. Dowling, Quantum Interferometric Optical Lithography: Exploiting Entanglement to Beat the Diffraction Limit, Phys. Rev. Lett. **85**, 2733 (2000).

[32] G. Y. Xiang, B. L. Higgins, D. W. Berry, H. M. Wiseman, and G. J. Pryde, Entanglement-enhanced measurement of a completely unknown optical phase, Nat. Photonics **5**, 43 (2010).

[33] K. Banaszek, R. Demkowicz-Dobrzanski, and I. A. Walmsley, Quantum states made to measure, Nat. Photonics **3**, 673 (2009).

[34] M. Kacprowicz, R. Demkowicz-Dobrzanski, W. Wasilewski, K. Banaszek, and I. A. Walmsley, Experimental quantum-enhanced estimation of a lossy phase shift, Nat. Photonics **4**, 357 (2010).

[35] H. Yonezawa, D. Nakane, T. A. Wheatley, K. Iwasawa, S. Takeda, H. Arao, K. Ohki, K. Tsumura, D. W. Berry, T. C. Ralph, H. M. Wiseman, E. H. Huntington, and A. Furusawa, Quantum-enhanced optical phase tracking, Science **337**, 1514 (2012).

[36] A. Monras, Optimal phase measurements with pure Gaussian states, Phys. Rev. A **73**, 033821 (2006).

[37] H. T. Dinani and D. W. Berry, Adaptive estimation of a time-varying phase with a power-law spectrum via continuous squeezed states, Phys. Rev. A **95**, 063821 (2017).

[38] W. H. Yang, X. L. Jin, X. D. Yu, Y. H. Zheng, and K. C. Peng, Dependence of measured audio-band squeezing level on local oscillator intensity noise, Opt. Express **25**, 24262 (2017).

[39] D. Li, B. T. Gard, Y. Gao, C. H. Yuan, W. P. Zhang, H. Lee, and J. P. Dowling, Phase sensitivity at the Heisenberg limit in an SU(1,1) interferometer via parity detection, Phys. Rev. A **94**, 063840 (2016).

[40] M. Aspachs, J. Calsamiglia, R. Muñz-Tapia, and E. Bagan, Phase estimation for thermal Gaussian states, Phys. Rev. A **79**, 033834 (2009).

[41] A. A. Berni, T. Gehring, B. M. Nielsen, V. Händchen, M. G. A. Paris, and U. L. Andersen, Ab initio quantum-enhanced optical phase estimation using real-time feedback control, Nat. Photonics **9**, 577 (2015).

[42] M. Proietti, M. Ringbauer, F. Graffitti, P. Barrow, A. Pickston, D. Kundys, D. Cavalcanti, L. Aolita, R. Chaves, and A. Fedrizzi, Enhanced Multiqubit Phase Estimation in Noisy Environments by Local Encoding, Phys. Rev. Lett. **123**, 180503 (2019).

[43] C. Zhang, T. R. Bromley, Y. Huang, H. Cao, W. Lv, B. Liu, C. Li, G. Guo, M. Cianciaruso, and G. Adesso, Demonstrating Quantum Coherence and Metrology That is Resilient to Transversal Noise, Phys. Rev. Lett. **123**, 180504 (2019).

[44] M. R. Huo, J. L. Qin, Y. R. Sun, J. L. Cheng, Z. H. Yan, and X. J. Jia, Generation of intensity difference squeezed state of light at optical fiber communication wavelength, Acta Sin. Quantum Opt. **24**, 134 (2018).

[45] M. Mehmet, S. Ast, T. Eberle, S. Steinlechner, H. Vahlbruch, and R. Schnabel, Squeezed light at 1550 nm with a quantum noise reduction of 12.3 dB, Opt. Express **19**, 25763 (2011).

[46] S. P. Shi, Y. J. Wang, W. H. Yang, Y. H. Zheng, and K. C. Peng, Detection and perfect fitting of 13.2 dB squeezed vacuum states by considering green-light-induced infrared absorption, Opt. Lett. **43**, 5411 (2018).

[47] H. Vahlbruch, M. Mehmet, K. Danzmann, and R. Schnabel, Detection of 15 dB Squeezed States of Light and Their Application for the Absolute Calibration of Photoelectric Quantum Efficiency, Phys. Rev. Lett. **117**, 110801 (2016).

[48] J. Sun, X. C. Zhang, W. Z. Qu, E. E. Mikhailov, I. Novikova, H. Shen, and Y. H. Xiao, Spatial Multiplexing of Squeezed Light by Coherence Diffusion, Phys. Rev. Lett. **123**, 203604 (2019).

[49] Y. Y. Zhou, J. Yu, Z. H. Yan, X. J. Jia, J. Zhang, C. D. Xie, and K. C. Peng, Quantum Secret Sharing among Four Players Using Multipartite Bound Entanglement of an Optical Field, Phys. Rev. Lett. **121**, 150502 (2018).

[50] N. Wiebe and C. Granade, Efficient Bayesian Phase Estimation, Phys. Rev. Lett. **117**, 010503 (2016).

[51] H. Cramér, *Mathematical Methods of Statistics* (Princeton University Press, Princeton, 1946).

[52] M. Hassani, C. Macchiavello, and L. Maccone, Digital Quantum Estimation, Phys. Rev. Lett. **119**, 200502 (2017).

[53] Y. Gao and H. Lee, Bounds on quantum multiple-parameter estimation with Gaussian state, Eur. Phys. J. D **68**, 347 (2014).

[54] R. Gaiba and M. G. A. Paris, Squeezed vacuum as a universal quantum probe, Phys. Lett. A **373**, 934 (2009).

[55] M. G. Genoni, S. Olivares, and M. G. A. Paris, Optical Phase Estimation in the Presence of Phase Diffusion, Phys. Rev. Lett. **106**, 153603 (2011).

[56] S. Grandi, A. Zavatta, M. Bellini, and M. G A Paris, Experimental quantum tomography of a homodyne detector, New J. Phys. **19**, 053015 (2017).

[57] M. R. Huo, J. L. Qin, J. L. Cheng, Z. H. Yan, Z. Z. Qin, X. L. Su, X. J. Jia, C. D. Xie, and K. C. Peng, Deterministic quantum teleportation through fiber channels, Sci. Adv. **4**, eaas9401 (2018).

[58] O. Pinel, P. Jian, N. Treps, C. Fabre, and D. Braun, Quantum parameter estimation using general single-mode Gaussian states, Phys. Rev. A **88**, 040102 (2013).

[59] S. Olivares and M. G. A. Paris, Bayesian estimation in homodyne interferometry, J. Phys. B: At. Mol. Opt. Phys. **42**, 055506 (2009).

[60] B. Chen, J. P. Geng, F. F. Zhou, L. L. Song, H. Shen, and N. Y. Xu, Quantum state tomography of a single electron spin in diamond with Wigner function reconstruction, Appl. Phys. Lett. **114**, 041102 (2019).

[61] U. Leonhardt, *Measuring the Quantum State of Light* (Cambridge University Press, Cambridge, 1997).

[62] M. G. A. Paris, Quantum estimation for quantum technology, Int. J. Quantum Inf. **7**, 125 (2009).

[63] Y. Y. Zhou, X. J. Jia, F. Li, C. D. Xie, and K. C. Peng, Experimental generation of 8.4 dB entangled state with an optical cavity involving a wedged type-II nonlinear crystal, Opt. Express **23**, 4952 (2015).

[64] X. W. Deng, S. H. Hao, H. Guo, C. D. Xie, and X. L. Su, Continuous variable quantum optical simulation for time evolution of quantum harmonic oscillators, Sci. Rep. **6**, 22914 (2016).